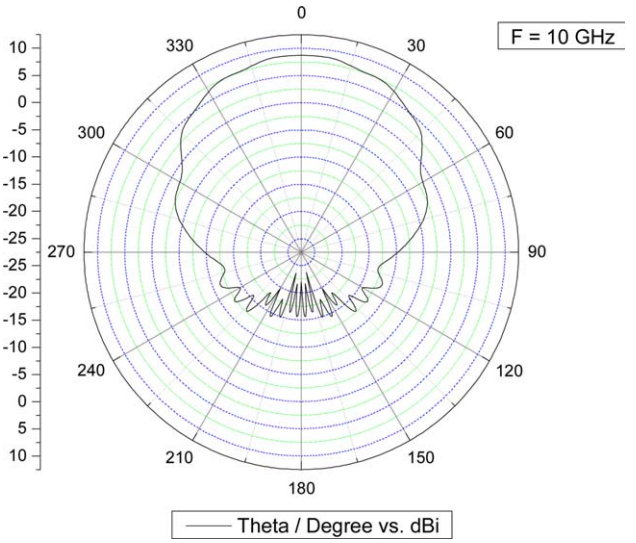

Figure 7 Radiation pattern (with defect) at frequency = 10 GHz. Directivity Abs (Phi = 90) Theta/Degree vs. dBi. [Color figure can be viewed in the online issue, which is available at wileyonlinelibrary.com]

entire bandwidth, the VSWR is reported to be ≤ 2. From this graph, the bandwidth calculated is about 1.2 GHz. The simulated radiation pattern for the antenna structure with defected ground at frequencies 10 GHz is shown in Figure 7. The polar plot of the radiation pattern is shown for directivity Abs (Phi = 90) between Theta/degree vs. dBi for the resonant frequency. At resonant frequency of 10 GHz (for Phi = 90), the antenna shows gain is 8.7 dBi in the main lobe direction 0.0°. Within 3-dB angular width in the direction 68.1° the side lobe level is −20.1 dB. The radiation pattern shows that a good antenna gain is obtained with improved radiation characteristics.

From all the above results, the simulated and experimentally measured return loss variation with the frequency and input impedance variation with the frequency for the DGS, it can be concluded that with the introduction of defect in the ground plane the impedance bandwidth increases with good impedance matching. The DGS is also very helpful in the overall size reduction of the antenna structure. With this, the radiation properties of the defected ground antenna structure are also improved to a very good extent as compared to the normal antenna structure.

4. CONCLUSION

A novel defected ground microstrip circular patch antenna is presented and tested. It has been observed that using the defected ground geometry and optimizing antenna parameter results in good impedance matching with high impedance bandwidth. The measured results are in good agreement with the experimental one. The designed antenna operates in the X-band in the frequency range 8–12 GHz giving a wide impedance bandwidth. It is also observed that a good antenna gain is obtained by introducing the defected ground plane. The bandwidth of the antenna enhanced, which is very good for wideband applications. The proposed antenna is applicable for various wideband communication systems especially working in the X-band.

REFERENCES

1. R. Garg, P. Bhartia, I. Behl, and A. Ittipiboon, Microstrip antenna design handbook, Artech House Inc., Norwood, MA, 2001.
2. H. Liu, Z. Li, and X. Sun, Compact defected ground structure in microstrip technology, Electron Lett 41 (2005), 132–134.
3. J.X. Liu, W.Y. Yin, and S.L. He, A new defected ground structure and its application for miniaturized switchable antenna, Prog Electromagn Res 107 (2010), 115–128.
4. M.K. Fries and R. Vahldieck, Small microstrip patch antenna using slow-wave structure, In: IEEE Antennas and Propagation Society International Symposium, Salt Lake City, UT, Vol. 1–4, July 2000, pp. 770–773.
5. L.-T. Wang and J.-S. Sun, The compact broadband microstip antenna with defective ground plane, In: IEEE International Conference on Antennas and Propagation, Vol. 2, Columbus, OH, April 2003, pp. 622–624.
6. S.H. Zainud-Deen, M.E. Badr, E. El-Deen, K.H. Awadallaand, and H.A. Sharshar, Microstrip antenna with defected ground plane structure as a sensor for landmines detection, Prog Electromagn Res B 4 (2008), 27–39.
7. J.S. Lim, C.S. Kim, Y.T. Lee, D. Ahn, and S. Nam, A spiral-shaped defected ground structure for coplanar waveguide, IEEE Microwave Wireless Compon Lett 12 (2002), 330–332.
8. L.H. Weng, Y.-C. Guo, X.-W. Shi, and X.-Q. Chen, An overview on defected ground structure, Prog Electromagn Res B 7 (2008), 173–189.
9. Y.B. Cho, K.S. Jun, and I.S. Kim, Small-size quasi-elliptic function microstrip low pass filter based on defected ground structures and open stubs, Microwave J 47 (2004).
10. G.H. Li, X.H. Jiang, and X.M. Zhong, A novel defected ground structure and its application to a low pass filter, Microwave Opt Technol Lett 48 (2006), 453–456.
11. A.K. Arya, M.V. Kartikeyan, and A. Patnaik, Efficiency enhancement of microstrip patch antennas with defected ground structure, In: IEEE International Conference on Recent Advances in Microwave Theory and Applications (MICROWAVE-08), November 2008, pp. 729–731.
12. A.K. Arya, M.V. Kartikeyan, and A. Patnaik, Neural network model for analysis of DGS structure, In: National Symposium on Vacuum Electronic Devices and Applications, (VEDA-2009), January 2009, pp. EMS1.1–EMS1.2.
13. C.S. Kim, J.S. Lim, S. Nam, K.Y. Kang, and D. Ahn, Equivalent circuit modeling of spiral defected ground structure for microstrip line, Electron Lett 38 (2002), 1109–1120.
14. E.K.I. Hamad, A.M.E. Safwat, and A.S. Omar, Controlled capacitance and inductance behaviour of L-shaped defected ground structure for coplanar waveguide, IEE Proc Microwave Antennas Propag 152 (2005), 299–304.
15. D. Guha, S. Biswas, M. Biswas, J.Y. Siddiqui, and Y.M.M. Antar, Concentric ring-shaped defected ground structures for microstrip applications, IEEE Antennas Wireless Propag Lett 5, 2006.

WWAN/LTE HANDSET ANTENNA WITH SHAPED CIRCUIT BOARD, BATTERY, AND METAL MIDPLATE

Kin-Lu Wong,[1] Hsuan-Jui Chang,[1] Fang-Hsien Chu,[1] Wei-Yu Li,[2] and Chun-Yih Wu[2]
[1] Department of Electrical Engineering, National Sun Yat-sen University, Kaohsiung 80424, Taiwan; Corresponding author: wongkl@ema.ee.nsysu.edu.tw
[2] Information and Communications Research Laboratories, Industrial Technology Research Institute, Hsinchu 31040, Taiwan

Received 13 February 2013

ABSTRACT: *An onboard printed WWAN/LTE antenna of simple structure disposed in a small clearance of 8 × 36 mm² in the ground plane of shaped circuit board in a slim handset is presented. The shaped circuit board has a large rectangular notch such that the battery of the handset can be embedded therein to decrease the thickness of the handset. It is shown that, compared to the traditional simple circuit board, the shaped circuit board can lead to much enhanced bandwidth of the antenna disposed thereon. This is mainly because stronger surface*

currents on the ground plane of the shaped circuit board can be excited, which greatly helps improve the operating bandwidth of the antenna disposed thereon. By properly short-circuiting the metal enclosing of the battery and the metal midplate that can be used to provide the handset with structural support, stronger excited surface currents on the ground plane of shaped circuit board can still be obtained. The proposed design makes a simple, small-size printed inverted-F antenna capable of providing two wide operating bands to cover the GSM850/900 bands (824–960 MHz) and GSM1800/1900/UMTS/LTE2300/2500 bands (1710–2690 MHz). Further, the proposed design can provide good antenna efficiency and meet the specific absorption rate regulations of less than 1.6 W/kg for 1-g head tissue as well. Detailed results of the proposed design are presented and discussed. © 2013 Wiley Periodicals, Inc. Microwave Opt Technol Lett 55:2254–2261, 2013; View this article online at wileyonlinelibrary.com. DOI 10.1002/mop.27835

Key words: *handset antennas; mobile antennas; shaped circuit board for bandwidth enhancement; wireless wide area network antennas; long term evolution antennas*

1. INTRODUCTION

Slim profile has been a trend for the handsets, especially for the smartphones. The slim handsets are generally with a thin profile of less than 10 mm. For the slim handset, the system circuit board therein may have a large rectangular notch or slot to accommodate the battery to decrease the total required thickness of the handset. In such cases, the shape of the ground plane on the system circuit board is varied accordingly. As it is well known that the ground plane on the system circuit board is also a part of the radiator [1–3], especially for the embedded antenna operated at lower frequencies [e.g., at about 900 MHz for the wireless wide area network (WWAN) operation], it is expected that the operating bandwidth and radiation efficiency of the antenna will be strongly affected by the shaped system circuit board in such slim handsets. In this study, we demonstrate that large bandwidth enhancement of an antenna disposed on the shaped system circuit board can be obtained, compared to that disposed on the traditional simple system circuit board.

In the proposed design, a battery generally having a metal enclosing is disposed in the large notch of the shaped circuit board. A metal midplate, which is used to provide the handset with structural support (e.g., the midplate can be used to support the display of the handset) [4], is also included in the proposed design. By connecting both the battery and metal midplate at proper locations to the ground plane of the shaped circuit board, large bandwidth enhancement for a small-size antenna can still be obtained.

The antenna used in this study is a simple, small-size printed inverted-F antenna, which can be disposed in a small clearance of 8×36 mm^2 in the ground plane of the shaped circuit board. In the proposed design, stronger surface currents excited on the ground plane of the shaped circuit board, compared to those on

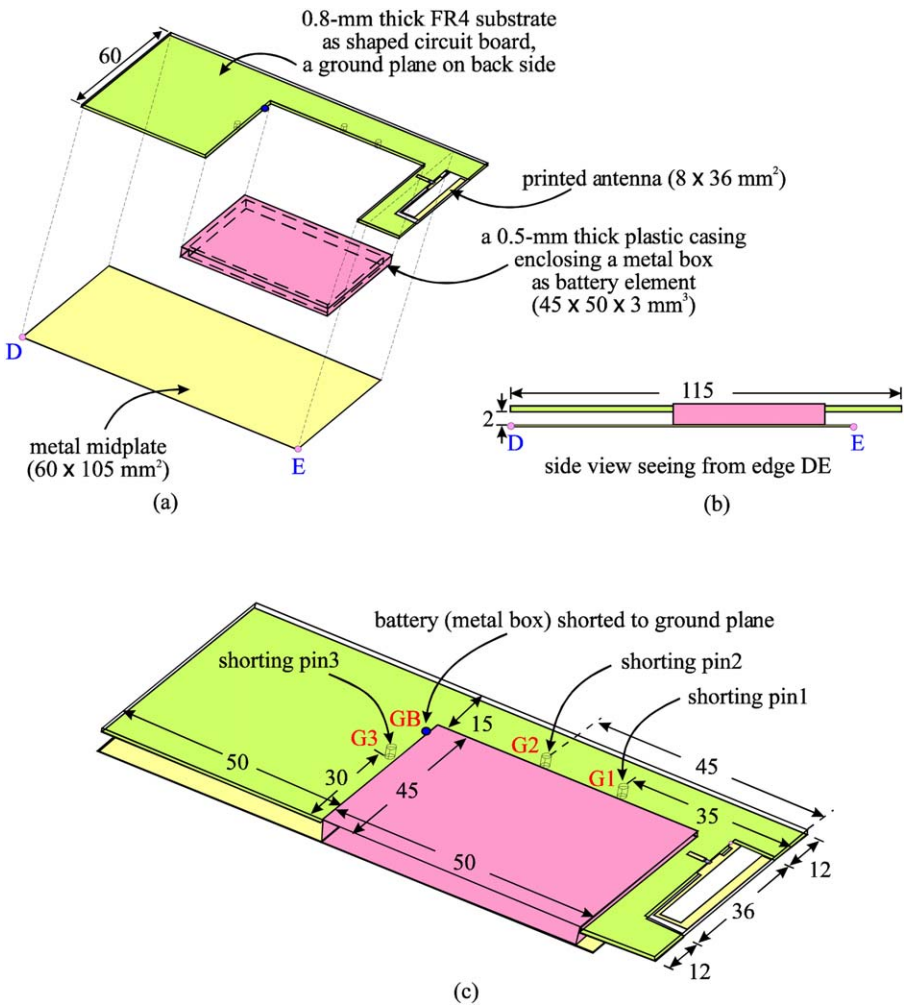

Figure 1 Proposed WWAN/LTE handset antenna with shaped circuit board, battery, and metal midplate. (a) Exploded view. (b) Side view. (c) Front view. [Color figure can be viewed in the online issue, which is available at wileyonlinelibrary.com]

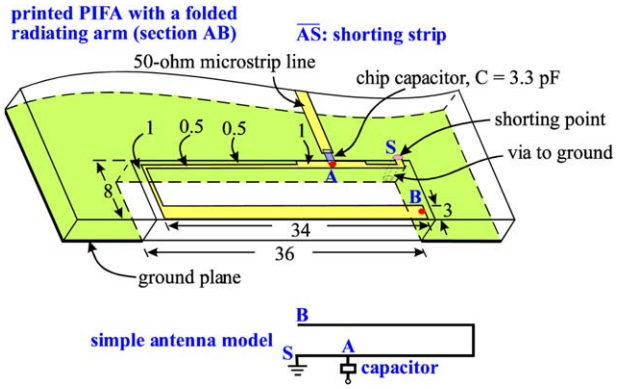

Figure 2 Dimensions of the metal pattern of the antenna (printed PIFA with a folded radiating arm). [Color figure can be viewed in the online issue, which is available at wileyonlinelibrary.com]

the ground plane of a corresponding simple circuit board, are observed. This behavior leads to enhanced bandwidth of the small-size antenna. Two wide operating bands are generated to cover the GSM850/900 bands (824–960 MHz) and GSM1800/1900/UMTS/LTE2300/2500 bands (1710–2690 MHz). That is, the WWAN and LTE (long term evolution) [5–7] operation can be covered using a simple, small-size onboard printed inverted-F antenna. The proposed design also shows good antenna efficiency and meets the specific absorption rate (SAR) regulations of less than 1.6 W/kg for 1-g head tissue [8,9] as well. Details of the proposed design are described. The proposed design was implemented, and obtained results are presented and discussed.

2. PROPOSED DESIGN

Figure 1 shows the geometry of the proposed design. As shown in Figure 1(a), there are three parts in the proposed design, which include a shaped circuit board with an onboard printed inverted-F antenna disposed thereon, a battery, and a metal midplate. The shaped circuit board is modeled using a 0.8-mm thick FR4 substrate of relative permittivity 4.4 and loss tangent 0.024. The width and length of the circuit board are, respectively, 60 and 115 mm, which are reasonable dimensions of practical smartphones. A ground plane is printed on the back side of the shaped circuit board. A large notch of size 45 $\times$ 50 mm^2 is cut in the circuit board to accommodate the battery of the handset. Note that the battery can have many different sizes (length, width, and thickness), depending on various battery lifetimes required for the handset. In practical cases, the notch size can be adjusted to accommodate the battery with various sizes, or the battery size can be adjusted to fit in the notch in the shaped circuit board. In this study, the shaped circuit board with a notch size which is reasonable for some practical handset batteries can have stronger surface currents excited on the ground plane thereof, compared to those on the ground plane of a corresponding simple circuit board. The simulated results of the excited surface currents on the ground plane will be discussed with the aid of Figure 9 in Section 3.

The antenna is printed on a small clearance of 8 $\times$ 36 mm^2 at the bottom edge of the shaped circuit board. As shown in Figure 2, the antenna has a folded radiating arm of length 66 mm (section AB) and a shorting strip of length 10 mm (section AS). The open-end portion of the radiating arm is widened (3-mm wide) to achieve better impedance matching for the antenna,

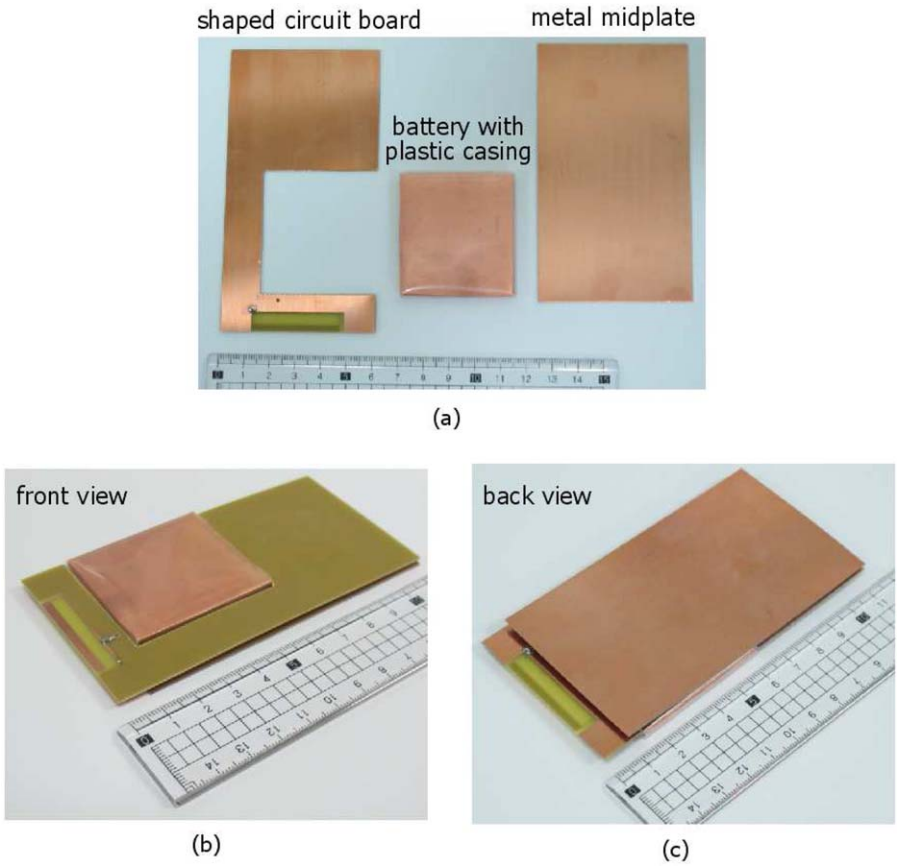

Figure 3 Photos of the fabricated prototype. (a) Shaped circuit board, battery element, and metal midplate. (b) Front view seeing from the battery side. (c) Back view seeing from the midplate side. [Color figure can be viewed in the online issue, which is available at wileyonlinelibrary.com]

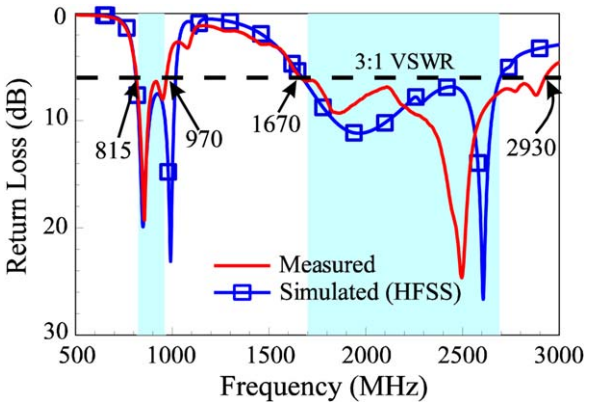

Figure 4 Measured and simulated return losses of the antenna. [Color figure can be viewed in the online issue, which is available at wileyonlinelibrary.com]

while other portions are with a width of 0.5 mm, except that (1-mm wide) near feeding point A. The portions of the shorting strip near feeding point A and shorting point S are also with a width of 1 mm, with other portion having a width of 0.5 mm. The portions with 1-mm width can decrease the fabrication errors for soldering in the experiment, whereas those with 0.5-mm width can increase the effective length of the radiating arm and shorting strip. A chip capacitor of 3.3 pF is added at feeding point A, which mainly compensates for large inductance for frequencies at about 900 MHz to achieve improved impedance matching for the antenna in this study. With the proposed design, two wide operating bands can be provided to cover the WWAN/LTE operation in the 824–960 and 1710–2690 MHz bands, although the antenna has a small size of 8×36 mm^2 only.

The battery is modeled as a metal box enclosed by a 0.5-mm thick plastic casing. The metal box is also short-circuited at the location GB to the ground plane of shaped circuit board. The location GB is at the edge of the battery opposite to the embedded antenna on the shaped circuit board. The selected location GB can make the excited surface currents on the ground plane of shaped circuit board slightly affected such that enhanced bandwidth of the antenna can still be obtained, when the battery is embedded in the notch of shaped circuit board.

The metal midplate is also considered in the proposed design. The midplate is usually added to provide the handset with structural support and can be used to support the display of the handset. In this study, the midplate is considered to be a metal plate and has a size of 60×105 mm^2, which is large enough for supporting the display (note that the display can be attached to the surface of the midplate that is opposite to the battery. To achieve a slim profile for the handset, a small distance of 2 mm between the midplate and the ground plane of shaped circuit board is selected. It should be noted that the 2-mm spacing between the midplate and the ground plane can be used to accommodate associated modules and circuits in the handset. The configuration of the proposed design can be seen more clearly in Figures 1(b) and 1(c). As the midplate is very close to the ground plane of shaped circuit board, it may cause large effects on the excited surface currents on the ground plane and decrease the operating bandwidth of the antenna. By properly selecting the shorting positions (G1, G2, and G3 in this study) to connect the midplate to the ground plane, the excited surface currents on the region of the midplate facing the battery (i.e., facing the notch of shaped circuit board) can be suppressed. Note that more shorting pins along the two edges of the notch as shown in Figure 1(c) will cause similar effects as obtained in this study. Hence, only three shorting positions of G1, G2, and G3 are used in the proposed design. This can lead to small effects on the excited surface currents on the ground plane of shaped circuit board. Hence, enhanced bandwidth can still be obtained for the small-size antenna in this study.

3. RESULTS AND DISCUSSION

The proposed design was implemented. The photos of the fabricated prototype are shown in Figure 3. In Figure 3(a), three parts in the proposed design are shown. The front and back views of the proposed design are shown in Figures 3(b) and 3(c), respectively. Figure 4 shows the measured and simulated return losses of the antenna. The simulated results are obtained using full-wave electromagnetic field simulator HFSS version 14 [10], and agreement between the simulation and measurement is seen. The obtained lower and upper bands of the antenna cover the WWAN (GSM850/900/1800/1900/UMTS) operation in the 824–960/1710–2170 MHz bands and the LTE2300/2500 operation in the 2300–2690 MHz bands. Over the operating bands, the impedance matching is better than 3:1 VSWR or 6-dB return loss, which is the design specification widely used for the internal WWAN/LTE handset antennas [11–13].

The measured antenna efficiency is shown in Figure 5. The antenna efficiency includes the mismatching loss. Over the lower band (824–960 MHz), the antenna efficiency is better than about 60%, whereas that over the upper band (1710–2690 MHz) is better than about 65%. The measured antenna efficiencies are good for practical handset applications. Figure 6 shows the measured three-dimensional total-power radiation patterns. Note that the antenna is disposed at the bottom edge of the shaped circuit board. This arrangement is generally applied in most smartphones to achieve decreased SAR values [14–16], which will be discussed with the aid of Figure 7. For the radiation patterns at lower frequencies (859 and 925 MHz), dipole-like patterns with omnidirectional radiation in the azimuthal plane (x-y plane) are seen. For frequencies in the upper band (1795, 2045, and 2595 MHz), more variations in the radiation patterns are seen and, however, strong radiation in the azimuthal plane is still observed. The observed radiation characteristics are acceptable for practical handset applications.

Figure 7 shows the SAR simulation model and the simulated SAR values for 1-g head tissue. The SAR simulation model is based on the SPEAG simulation software SEMCAD X version

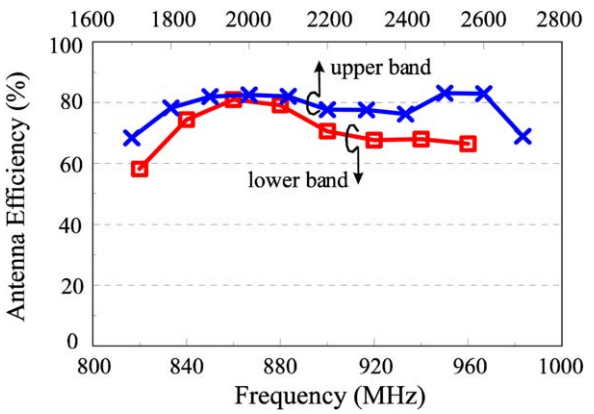

Figure 5 Measured antenna efficiency with mismatching loss. [Color figure can be viewed in the online issue, which is available at wileyonlinelibrary.com]

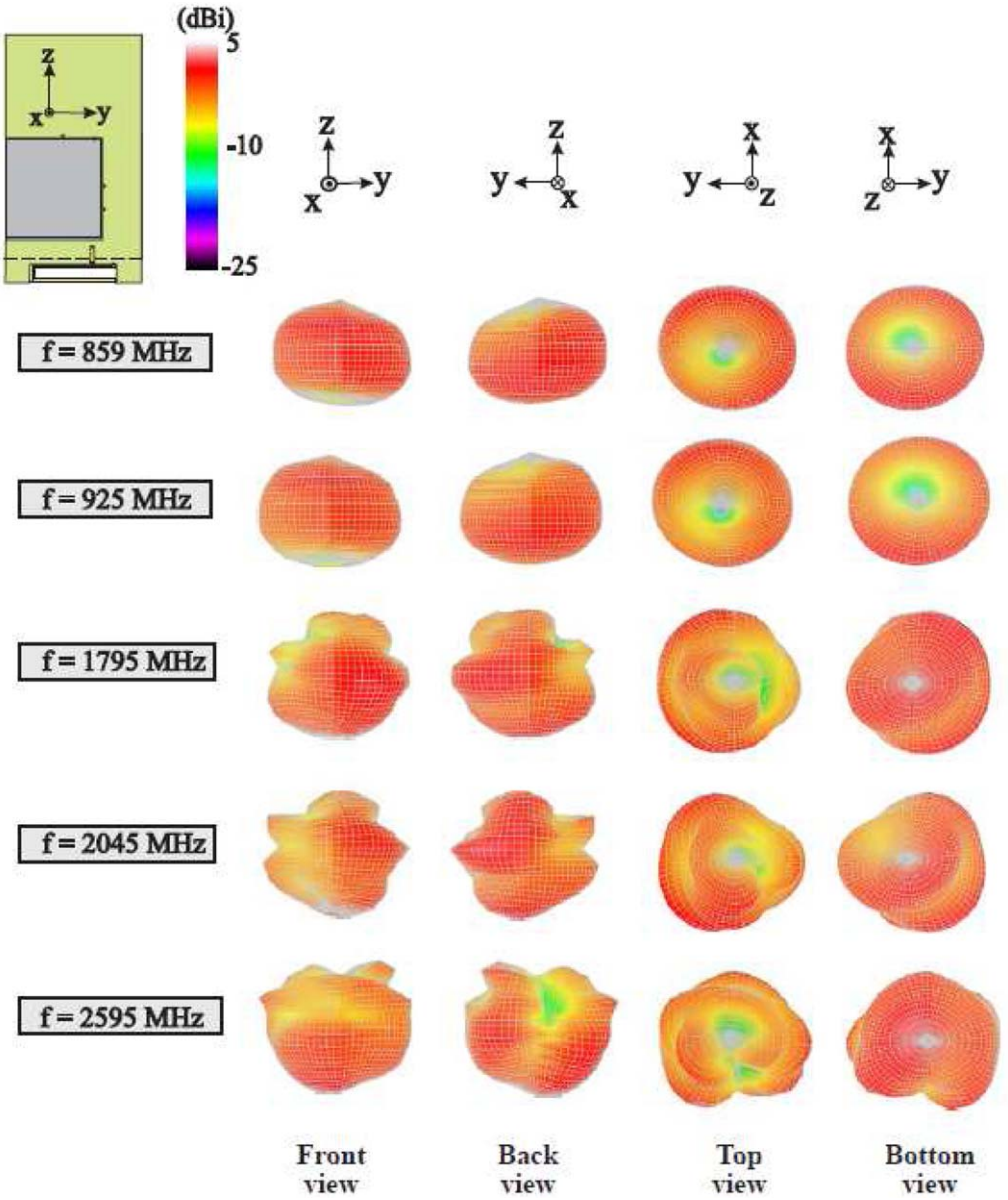

Figure 6 Measured three-dimensional total-power radiation patterns of the antenna. [Color figure can be viewed in the online issue, which is available at wileyonlinelibrary.com]

14 [17]. The handset with the proposed design is attached to right cheek of the phantom head (the dashed line indicates the possible casing for the handset), and the 3-mm spacing is between the metal midplate and the phantom head. The 3-mm spacing can be considered as the thickness of the display attached to the metal midplate. The testing power and the return loss of the antenna at the testing frequencies are also given in the figure. The return losses at the testing frequencies are all better than 6 dB, when the phantom head is attached to the handset with the proposed design. It is seen that the obtained 1-g SAR values at representative frequencies all meet the SAR regulation of less than 1.6 W/kg [8].

Figure 8 shows the simulated return loss for the case with a simple circuit board (Ant1), the case with a shaped circuit board (Ant2), the case with a shaped circuit board and a metal midplate (Ant3), and the proposed design. The antenna dimensions are the same in all cases, while the notch size in Ant2 is adjusted to be 35×50 mm^2, different from those (all 45×50 mm^2) in the proposed design, Ant1 and Ant3, to achieve optimal impedance matching in each case to have a fair comparison. Results indicate that for Ant1, its lower-band bandwidth is small and far from covering the GSM850/900 bands. For Ant2 with the shaped circuit board, enhanced bandwidths in the antenna's lower and upper bands are obtained. This behavior may be explained from the excited surface current distributions shown in Figure 9, in which it is seen that strong surface currents on the portion adjacent to the notch in the longitudinal direction are seen for Ant2, especially at lower frequency (925 MHz). This behavior leads to enhanced bandwidth for Ant2. It is also noted that Ant2 has a much widened upper-band bandwidth with the frequencies therein having improved impedance matching. The first mode at about 1.6 GHz in Ant2's upper band is related to the resonant mode at about 1.9 GHz in Ant1's upper band, which is a higher-order mode of the printed inverted-F antenna. The frequency shifting is due to the presence of the notch in the shaped circuit board. The second mode at about

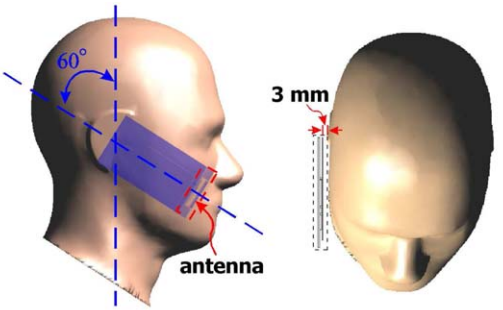

Frequency (MHz)	Testing power (dBm)	SAR_{1g} (W/kg)	Return loss (dB)
859	24	1.35	24.5
925	24	1.26	8.0
1795	21	0.45	9.7
1920	21	0.42	9.2
2045	21	0.38	8.5
2350	21	0.37	6.1
2595	21	0.46	12.0

Figure 7 SAR simulation model and the simulated SAR values for 1-g head tissue. [Color figure can be viewed in the online issue, which is available at wileyonlinelibrary.com]

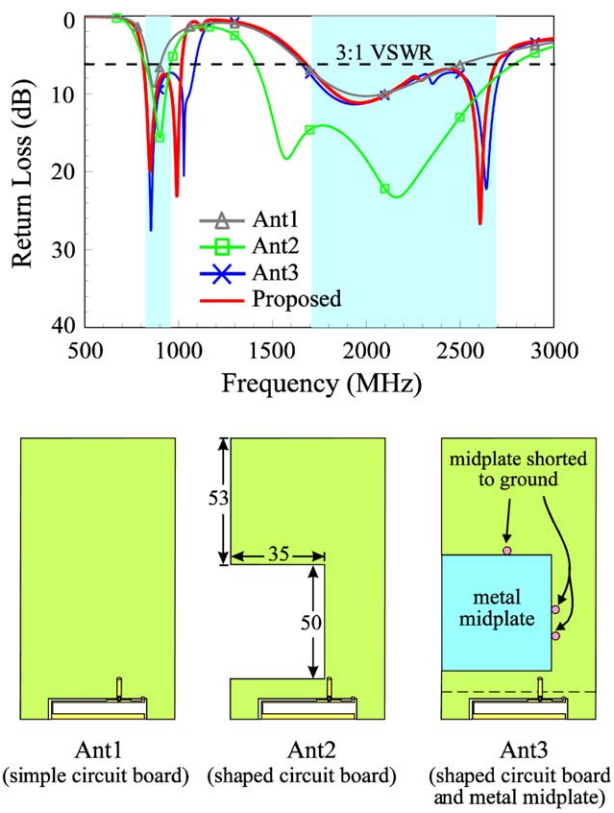

Figure 8 Simulated return loss for the case with a simple circuit board (Ant1), the case with a shaped circuit board (Ant2), the case with a shaped circuit board and a metal midplate (Ant3), and the proposed design. [Color figure can be viewed in the online issue, which is available at wileyonlinelibrary.com]

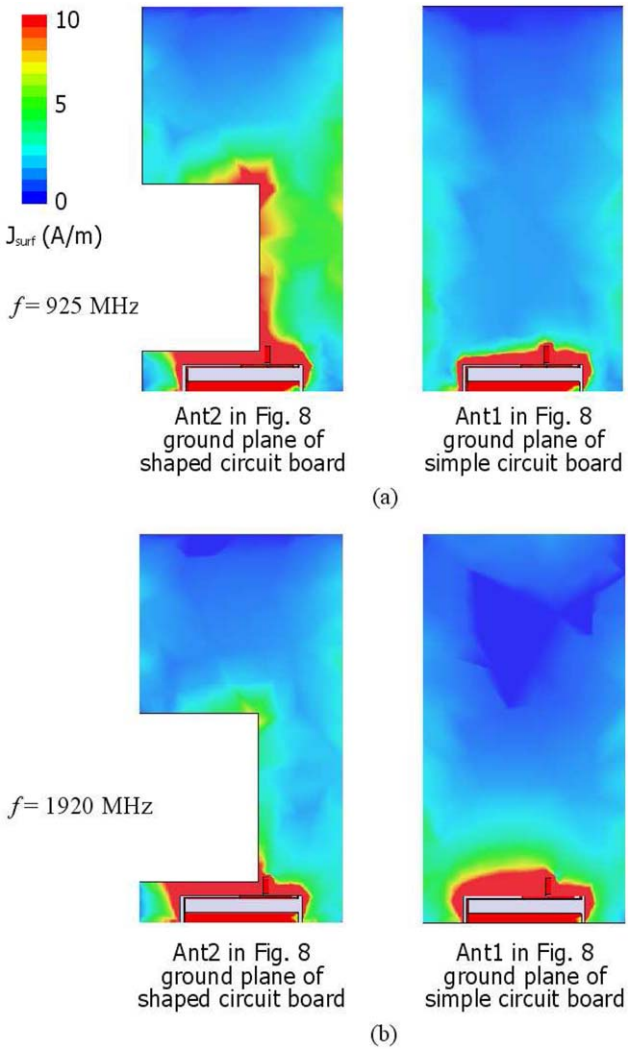

Figure 9 Simulated surface current distributions on the ground plane of shaped circuit board (Ant2 in Fig. 8) and on the ground plane of simple circuit board (Ant1 in Fig. 8). (a) $f = 925$ MHz. (b) $f = 1920$ MHz. [Color figure can be viewed in the online issue, which is available at wileyonlinelibrary.com]

2.2 GHz in Ant2's upper band is very likely related to an efficient resonant path along the ground portion around the notch being created, which greatly enhances the antenna's upper-band bandwidth.

For Ant3 with the metal midplate added and connected to the ground plane at proper positions, effects on the excited surface current distributions on the ground plane of shaped circuit board can be minimized. By further adding the battery to be embedded inside the notch of shaped circuit board and connecting the metal enclosing of the battery at a proper position to the ground plane to form the proposed design, strong surface currents on the portion adjacent to the notch in the longitudinal direction can still be obtained. Hence, widened bandwidth in the lower band is also obtained for Ant3 and proposed design, as compared to the bandwidth of Ant1. This can also be explained by using the excited surface current distributions shown in Figure 10 for the proposed design, in which it is seen that both the battery's metal enclosing and the region of the metal midplate facing the battery show very weak current distributions. In this case, on the ground plane of shaped circuit board, strong surface currents on the portion adjacent to the notch in the longitudinal direction are still obtained. This leads to wider

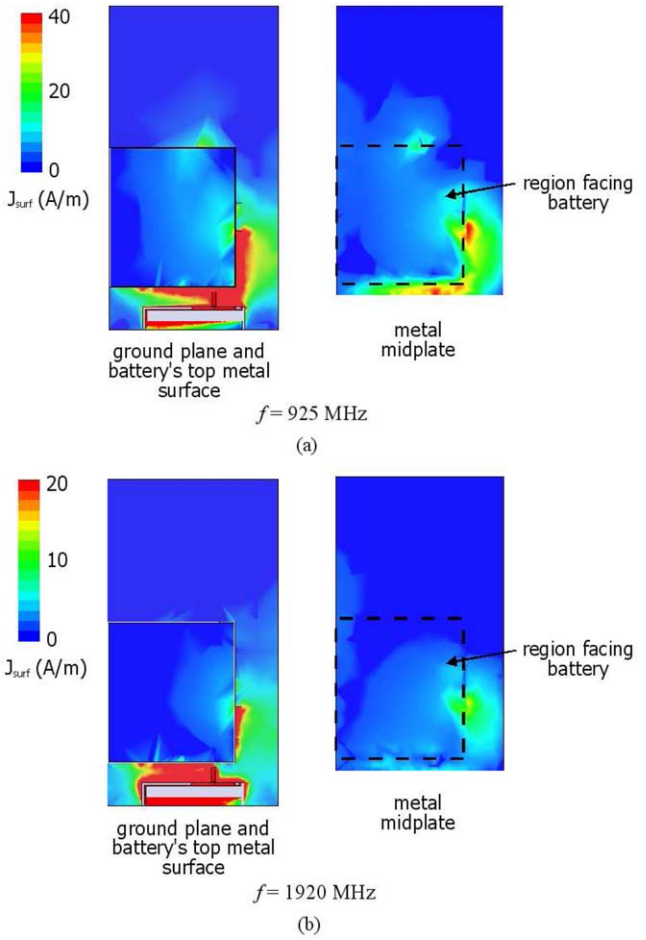

Figure 10 Simulated surface current distributions on the ground plane of shaped circuit board, battery's top metal surface and metal midplate for the proposed design. (a) $f = 925$ MHz. (b) $f = 1920$ MHz. [Color figure can be viewed in the online issue, which is available at wileyonlinelibrary.com]

bandwidth obtained for the proposed design, especially for the lower-band bandwidth. Also note that, in Figure 8, the higher-order mode of the printed PIFA at about 1.9 GHz is not shifted (Ant3 and proposed design vs. Ant1), which is probably because with the metal midplate added, a complete circuit board is seen at higher frequencies for the antenna and thus, makes the antenna's higher-order mode show similar behavior as that of Ant1. However, a resonant mode at about 2.6 GHz is seen for Ant3 and proposed design. This additional resonant mode is related to the metal midplate connected at proper positions to the ground plane.

Effects of different connections between the metal midplate and ground plane are also analyzed. Figure 11 shows the simulated return loss for the case with a floating metal midplate (Ant4), the case with the metal midplate short-circuited at its four corners to the ground plane of shaped circuit board (Ant5), and the proposed design. For Ant4 and Ant5, it is seen that the obtained bandwidths, especially the lower-band bandwidth, are greatly decreased, as compared to the proposed design. This is mainly because, when there are no connections or the connection positions are not properly selected, the excited surface currents on the ground plane of shaped circuit board will be greatly varied, which will lead to degraded impedance matching for frequencies in the desired operating bands. The operating bandwidth of the antenna will hence be greatly decreased.

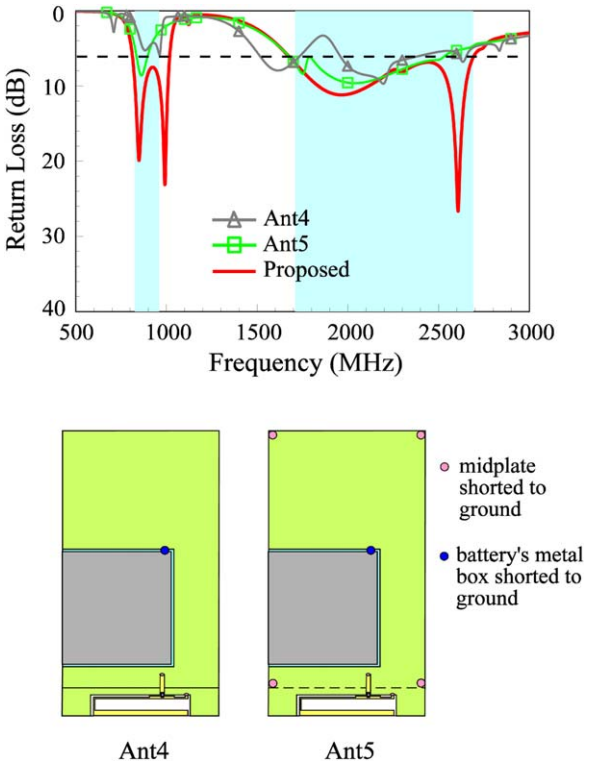

Figure 11 Simulated return loss for the case with a floating metal midplate (Ant4) and the case with the metal midplate short-circuited at its four corners to the ground plane of shaped circuit board (Ant5), and the proposed design. [Color figure can be viewed in the online issue, which is available at wileyonlinelibrary.com]

Finally, it is shown in Figure 12 that the chip capacitor of 3.3 pF added at the feeding point of the antenna can effectively compensate for the large inductance seen around 900 MHz in the antenna's lower band. With the chip capacitor added, it is seen that the peak value of the real input resistance at about 900 MHz decreases to be close to 50 Ω. This helps in obtaining

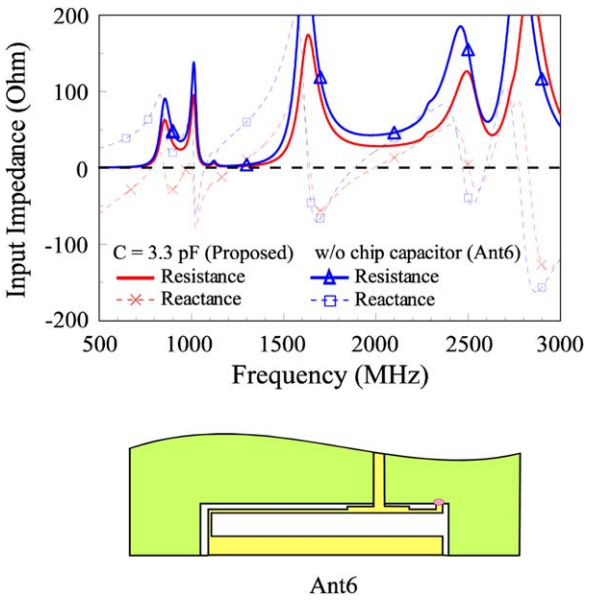

Figure 12 Simulated return loss for the antenna with and without a chip capacitor at the feeding point. [Color figure can be viewed in the online issue, which is available at wileyonlinelibrary.com]

improved impedance matching for frequencies in the desired operating bands of the proposed design.

4. CONCLUSION

A simple, small-size printed inverted-F antenna has been shown to provide wide operating bands to cover the WWAN and LTE operation in the 824–960 and 1710–2690 MHz bands for the slim handset application. The antenna is disposed in a small clearance of a shaped circuit board, and the wideband operation is obtained mainly owing to the ground plane on the shaped circuit board excited to be an efficient radiator. To make it more promising for practical slim handset application, a battery embedded in the notch of the shaped circuit board and a metal midplate for the structural support of the handset are added and connected at proper positions to the ground plane of shaped circuit board. The proposed design can still have the ground plane of shaped circuit board excited as an efficient radiator to greatly enhance the operating bandwidth of the antenna. Good far-field radiation characteristics for frequencies in the operating bands have also been obtained. In addition, the simulated SAR values for 1-g head tissue are all less than 1.6 W/kg, meeting the SAR regulation for practical handset applications. The proposed design is especially suitable for the slim handset application.

REFERENCES

1. T.Y. Wu and K.L. Wong, On the impedance bandwidth of a planar inverted-F antenna for mobile handsets, Microwave Opt Technol Lett 32 (2002), 249–251.
2. P. Vainikainen, J. Ollikainen, O. Kivekas, and I. Kelander, Resonator-based analysis of the combination of mobile handset antenna and chassis, IEEE Trans Antennas Propag 50 (2002), 1433–1444.
3. A. Cabedo, J. Anguera, C. Picher, M. Ribo, and C. Puente, Multiband handset antenna combining a PIFA, slots, and ground plane modes, IEEE Trans Antennas Propag 57 (2009), 2526–2533.
4. M. Pascolini, R.W. Schlub, R. Caballero, N. Jin, and S. Myers, Housing structures for optimizing location of emitted radio-frequency signals, US Patent publication No. 2011/0291896 A1, December 1, 2011.
5. Q. Rao and D. Wang, A compact dual-port diversity antenna for long-term evolution handheld devices, IEEE Trans Veh Technol 59 (2010), 1319–1329.
6. K.L. Wong, M.F. Tu, C.Y. Wu, and W.Y. Li, On-board 7-band WWAN/LTE antenna with small size and compact integration with nearby ground plane in the mobile phone, Microwave Opt Technol Lett 52 (2010), 2847–2853.
7. K.L. Wong, T.W. Kang, and M.F. Tu, Antenna array for LTE/WWAN and LTE MIMO operations in the mobile phone, Microwave Opt Technol Lett 53 (2011), 1569–1573.
8. American National Standards Institute (ANSI), Safety levels with respect to human exposure to radio-frequency electromagnetic field, 3 kHz to 300 GHz, ANSI/IEEE standard C95.1, April 1999.
9. Y.W. Chi and K.L. Wong, Quarter-wavelength printed loop antenna with an internal printed matching circuit for GSM/DCS/PCS/UMTS operation in the mobile phone, IEEE Trans Antennas Propag 57 (2009), 2541–2547.
10. ANSYS Corporation High Frequency Structure Synthesizer (HFSS), Available at http://www.ansys.com/products/hf/hfss/, ANSYS Corporation, Pittsburgh, PA.
11. C.T. Lee and K.L. Wong, Planar monopole with a coupling feed and an inductive shorting strip for LTE/GSM/UMTS operation in the mobile phone, IEEE Trans Antennas Propag 58 (2010), 2479–2483.
12. K.L. Wong, Y.W. Chang, and S.C. Chen, Bandwidth enhancement of small-size WWAN tablet computer antenna using a parallel-resonant spiral slit, IEEE Trans Antennas Propag 60 (2012), 1705–1711.
13. C.L. Liu, Y.F. Lin, C.M. Liang, S.C. Pan, and H.M. Chen, Miniature internal penta-band monopole antenna for mobile phones, IEEE Trans Antennas Propag 58 (2010), 1008–1011.
14. C.H. Li, E. Ofli, N. Chavannes, and N. Kuster, Effects of hand phantom on mobile phone antenna performance, IEEE Trans Antennas Propag 57 (2009), 2763–2770.
15. K.L. Wong, W.Y. Chen, and T.W. Kang, On-board printed coupled-fed loop antenna in close proximity to the surrounding ground plane for penta-band WWAN mobile phone, IEEE Trans Antennas Propag 59 (2011), 751–757.
16. C.H. Chang and K.L. Wong, Printed $\lambda/8$-PIFA for penta-band WWAN operation in the mobile phone, IEEE Trans Antennas Propag 57 (2009), 1373–1381.
17. Schmid & Partner Engineering AG (SPEAG), SEMCAD, Available at http://www.semcad.com, Schmid & Partner Engineering AG (SPEAG).

EFFICIENT CLOSED-FORM GREEN'S FUNCTIONS FOR LAYERED STRIPLINE STRUCTURES

Jun Dingand and Steven L. Dvorak
Department of Electrical and Computer Engineering, University of Arizona, 1230 E Speedway Blvd., Tucson, AZ 85721; Corresponding author: sldvorak@email.arizona.edu

Received 21 February 2013

ABSTRACT: *In this article, simple and efficient closed-form Green's function representations for various inhomogeneously-filled (layered) stripline structures are derived in terms of cylindrical and spherical waves for a horizontal electric dipole source. The method is based on a two-level approximation of the spectral-domain Green's function. After using a fast pole-location method to extract the surface-wave modes that are guided by the dielectric slabs and the parallel-plate modes that are trapped by the two ground planes, we first use a method that is similar to the first step in the traditional two-level discrete complex image method (DCIM). This step provides a good approximation to the spectral-domain Green's function for large values of the spectral variable k_ρ, thus accounting for the fields at near and intermediate distances from the source. The remainder (smaller values of k_ρ) of the spectral-domain Green's function is approximated using a few poles and residues by using the total least squares algorithm, which requires much less computational resources as compared to the vector fitting method or DCIM. This portion of the Green's function accounts well for the fields that are further away from the source. Our proposed method provides an efficient and accurate means for representing Green's functions in layered stripline structures both near and far from the source. The results are verified by comparing with those obtained using the traditional two-level DCIM as well as direct numerical integration of the spectral-domain Green's function.* © 2013 Wiley Periodicals, Inc. Microwave Opt Technol Lett 55:2261–2265, 2013; View this article online at wileyonlinelibrary.com. DOI 10.1002/mop.27815

Key words: *Green's function; stripline structure; total least squares algorithm*

1. INTRODUCTION

The mixed potential integral equation (MPIE) formulation is often used together with the method of moments to solve for electromagnetic fields in layered microstrip and stripline structures. The evaluation of the spatial-domain Green's function plays a critical role in the MPIE method. Various methods have been developed for evaluating the Green's function in the past several decades. Among these methods, there are numerical methods like the generalized weighted average and double exponential methods, and analytical methods like the discrete